J Mater Sci (2010) 45:4462–4469
DOI 10.1007/s10853-010-4529-x

Characterization of rigid polyurethane foams containing microencapsulated Rubitherm® RT27. Part I

Ana M. Borreguero · José L. Valverde · Ton Peijs · Juan F. Rodríguez · Manuel Carmona

Received: 2 March 2010 / Accepted: 13 April 2010 / Published online: 1 May 2010

Abstract Rigid polyurethane foams (RPU foams) and phase change materials (PCMs) are widely used in buildings for thermal insulation and thermal storage, respectively. The combination of both materials could increase energy savings, leading to more energy efficient housing. In this work, PU foams were produced incorporating different percentages of microcapsules containing Rubitherm® RT27. Microcapsules added to the foam had a high influence on the foaming process and also on the foam properties. It was observed that the increase of foam microcapsules content decreases the final foam height but increases its density and thermal energy storage (TES) capacity. On the other hand, an increase of the foam microcapsules content up to 5 wt% led to decrease the reduced compressive strength (RS) and modulus (RE) in 7 and 25%, respectively. Higher contents had a sharply negative impact on mechanical properties.

Introduction

The constant increase of the energy demand and consequently of the air pollution is promoting the use of renewable energies and the development of new systems for saving energy. According to the EU directive 2002/91/EC, more than 40% of the final energy consumption in the Europe Community in 2002 was due to the residential and tertiary sector. This energy was mainly spent for buildings comfort and this consumption increases day by day with its subsequent contribution to global warming by the carbon dioxide emissions associated with it.

Rigid polyurethane foams (RPU foams) are widely used as insulating materials in buildings due to their low thermal conductivity and high mechanical and chemical stabilities [1]. The synthesis of PU foams is basically based on the condensation reaction between diols or polyols and diisocyanates or polyisocyanates in presence of a catalyst. Blowing agents and surfactants are added to regulate the morphology of the foam cells [2].

As commented above, PU foams have good insulating properties but their thermoregulation capacity can be enhanced by incorporating phase change materials (PCMs) [3]. PCMs are materials that can absorb or release the energy equivalent with their latent heat when the temperature undergoes or overpasses the phase change temperature of the material.

In a previous work, the effect of microencapsulated Rubitherm® RT27 on the thermal energy storage (TES) capacity of gypsum blocks has been studied and the results indicated that the higher the microcapsule contents, the higher the amount of TES and also, the building insulation [4]. Thus, microcapsules containing PCMs can be used to modify the TES capacity of PU foams and holding the foam insulating properties.

The incorporation of PCMs into the building materials can be carried out by direct or indirect way. Sarier and Onder [1] studied the direct incorporation of *n*-hexadecane, *n*-hexadecane/$Na_2CO_3{\cdot}10H_2O$, *n*-octadecane and *n*-octadecane/PEG600 as PCMs to PU foams changing the mass ratio PCM/PU in the mixture from 1:5 to 1:1. They found that PCMs enhance the foam TES capacity; however, some

A. M. Borreguero · J. L. Valverde · J. F. Rodríguez · M. Carmona (✉)
Department of Chemical Engineering, University of Castilla-La Mancha, Av. Camilo José Cela s/n, 13004 Ciudad Real, Spain
e-mail: manuel.cfranco@uclm.es

T. Peijs
School of Engineering and Materials Science, Queen Mary University of London, Mile End Road, London E1 4NS, UK

leakage was observed when *n*-hexadecane was used. This problem was attributed to the small size of the *n*-hexadecane molecule that can escape from the cells. You et al. [5] found a large influence of the microencapsulated PCMs on the foaming system compared to that of another filler such as $CaCO_3$, $CaSO_4$ or hollow glass microspheres, even at low concentration. They justify this behaviour attending to the additives used in the microcapsule synthesis which have hydroxyl groups with a high ability for water absorption. Besides, they found that fillers affect the surface tension and viscosity of the foaming system, having a negative effect on the foam product. In the same way, Ye et al. [6] found that a large size of the filler or a poor interfacial adhesion between the filler and the foam matrix can cause collapse of the cells reducing the mechanical properties of the RPU foams. Although microencapsulated PCMs has been previously incorporated into PU foams [5, 7], studies of microcapsules distribution into the foam, their location in cells or struts and also their effect on the foam mechanical properties has not yet been considered. Besides, for the further building applications, it is important to know the effect of the PCMs on the density and foaming of the RPU foams and thus, a simple model that allows to know the influence of the filler on the foam rising has been developed.

The goal of this work is to study the incorporation of microcapsulated Rubitherm® RT27 as fillers into RPU foams synthesized using Tegoamin BDE as catalyst. The foaming process and the physical and mechanical properties of the final product were analysed.

Experimental

Materials

Polyol used in this work was Alcupol R-458 from Repsol YPF S.A. Diphenylmethane-4,4′-diisocyanate (MDI) was supplied by Merck Group. The catalyst used was Tegoamin BDE and the surfactant was Tegostab B8404, both supplied by Evonik Degussa International AG. Deionized water was used as a blowing agent. Spherical microcapsules containing Rubitherm® RT27 with a particle size ranging between 1 and 5 μm were obtained following the method described in the Patent EP2119498 [8].

PU foams synthesis

RPU foams were synthesized by weighting and mixing desired masses of polyol, silicone, water, amine and microcapsules containing Rubitherm® RT27 and further stirring the mixture during 1 min. Then, the adequate quantity of isocyanate was added to the mixture and the resulting solution was stirred for just 5 s until the moment at which the foam started to grow up. Finally, the obtained foams were cured at room temperature. Table 1 shows the foam synthesis recipe.

Table 1 Weight percentage of raw materials for PU foams synthesis

	Weight percentage
Polyol	48.43
Water	1.21
Silicone	0.73
Amine	1.21
MDI	48.43

Sample characterization

Rising process

The foams rising process was measured by an ultrasonic system sqs-01 recording the foam height with time by using the program Schaum SQS-01.

Microcapsules distribution and average latent heat of foams

The whole foam microcapsules distribution was studied by DSC analysis of samples taken out at different points. Samples were of cubic shape with a weight close to 6.0 mg. The microcapsules presence and its amount into the foam can be obtained by the peak size observed at the PCM melting point. Figure 1 shows the foam locations studied. DSC analyses were performed in the range from −10 to 45 °C at a heating rate of 5 °C/min. Each analysis was done twice.

SEM analysis

Synthesized RPU foams were depicted by SEM to visualize the possible changes in their cellular structure when

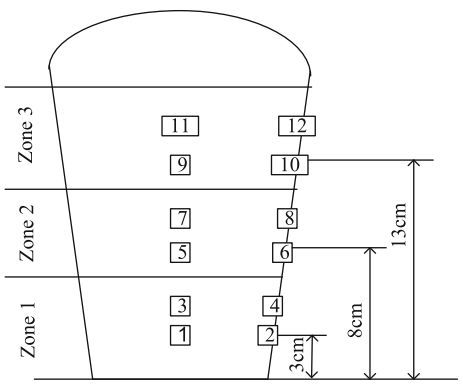

Fig. 1 Distribution of the analyzed points for studying the microcapsules distribution in the PU foams

different amounts of microcapsules are added and the foam cellular size distribution was determined by the Image Plus program.

Density

Foam densities were calculated by weighting and measuring the volume of the samples taken out.

Compression test

Uniaxial compression tests were performed according to ASTM D1621 using the Model 5584 of an INSTRON universal testing instrument equipped with a 1 kN load cell. The compression tests were carried out at a cross-head speed of 2.5 mm/min and transversal to the rising direction. The tested foam specimens were 5.1 × 5.1 × 2.6 cm size and they were compressed 13% of their original thickness. Each analysis was repeated 3 times. The foam compression strength (S) was obtained using the force required to get a 10% of specimen deformation and the compressive modulus (E) was calculated dividing the slope of the force–deformation curves obtained below the proportional limit by the area of the specimen and multiplying the result by the initial height.

Results

Foam growth

As can be seen in Fig. 2, the foaming rate decreases with increasing microcapsules content, since a lower slope of the curve at the short time region is observed. Besides, this figure shows that the higher the microcapsules content, the lower the final foam height. A similar behaviour was obtained by Verdejo et al. [9] when carbon nanotubes (CNTs) were incorporated to PU foams. They observed that the incorporation of CNTs either increased the viscosity of the foaming system limiting the foam expansion or substituting urethane linkages by CNTs, promoting a gelation process during the foaming. Thus, filler addition promotes higher viscosities of the foaming system what justifies the lower rising rates and final foam heights obtained.

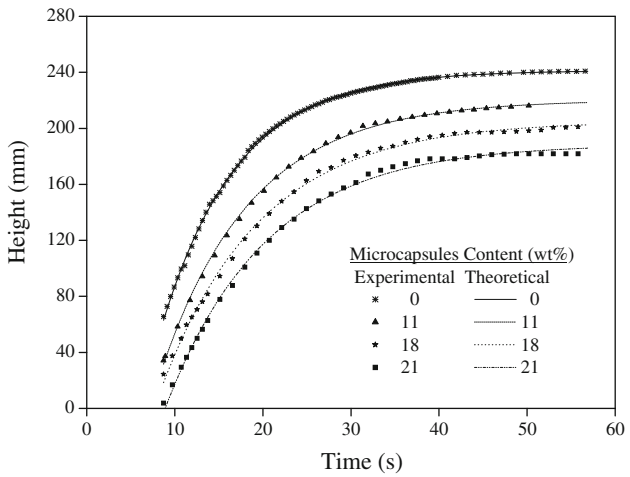

Fig. 2 Experimental and theoretical rising curves of the PU foams for different microcapsules contents

For the further building applications, it is important to know the effect of the PCMs on the RPU foaming. Several authors approached the rising process of PU foams to kinetic reactions of first- or second-order [10–12]. However, the application of these kinetic equations has some limits because the rising process involves many phenomena including mixing, chemical reaction, bubble growth and heat and mass transports; being complex to consider all them simultaneously [12]. In order to simplify the complexity of this process, in this work the experimental data of the rising of foams were fitted using a model of reaction curve of first-order with dead time, assuming that the addition of isocyanate can be represented as a step change of this process and the foam height is registered as an output variable (h). The transfer function that represents the above model is shown in Eq. 1 [13].

$$\frac{H(s)}{X(s)} = \frac{K \cdot e^{-\theta \cdot s}}{\tau \cdot s + 1} \tag{1}$$

where K is the maximum change of h for a unitary step change of the inlet variable x, τ is the time constant and θ is the dead time.

Applying the inverse Laplace transform, Eq. 1 becomes:

$$h(t) = K \cdot \left[1 - e^{\frac{t-\theta}{\tau}}\right] \tag{2}$$

The fitting parameters (K, τ and θ) were obtained minimizing the sum of the square of offsets by means of nonlinear least square fitting. This fitting process was carried out using the *solver* tool in Excel.

As can be seen in Fig. 2, a good agreement between the experimental data and the reaction curves using the model of first-order with dead time was obtained. A linear relationship between the parameters of the model and the microcapsules content was observed (Fig. 3). This linear relationship based on three parameters with respect to the weight percentage is expressed by Eq. 3.

$$y_i = a_i + b_i \cdot w_{\mathrm{PCM}} \tag{3}$$

where y is each of the three fitting parameters (K, τ and θ), a and b are constants of the linear equation, w_{PCM} is the

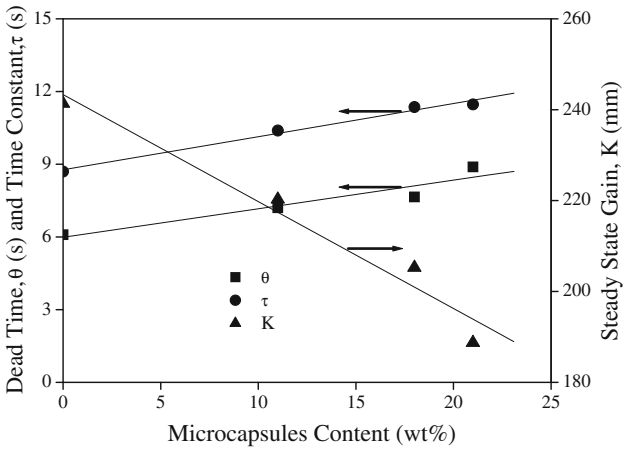

Fig. 3 Influence of the microcapsules content on the fitting parameters of the rising equations of the foams

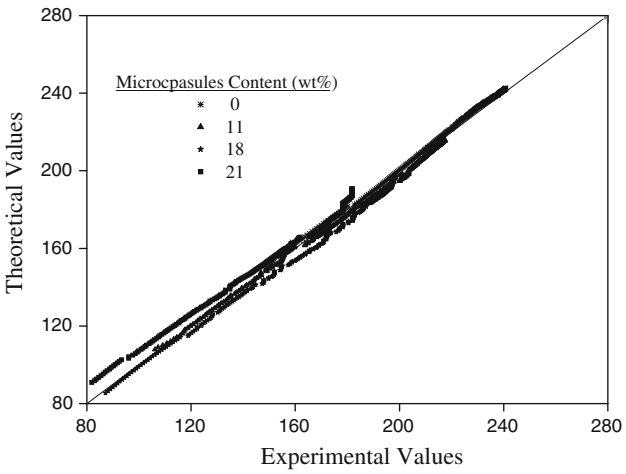

Fig. 4 Relationship between the experimental and theoretical data predicted by Eq. 4

Table 2 Parameters and coefficients of determination (R^2) for fitting the foam height with the microcapsules content

Parameters	Units	Value	R^2
a_0	mm	243.312	0.962
b_0	mm/wt_{PCM}%	−2.353	
a_1	s	5.988	0.898
b_1	s/wt_{PCM}%	0.118	
a_2	s	8.770	0.987
b_2	s/wt_{PCM}%	0.137	

n^{exp} is the number of experimental data considered, h^{exp}, h^{theo} and $\overline{h^{exp}}$ are the experimental, theoretical and average foam heights, respectively. R^2 was obtained by: $R^2 = 1 - \left\{ \left(\sum_{i=1}^{n^{exp}} (h^{exp} - h^{theo})^2 \right) \Big/ \left(\sum_{i=1}^{n^{exp}} (h^{exp} - \overline{h^{exp}})^2 \right) \right\}$

content of PCM in the foam in percentage by weight and i is a counter that represents each fitting parameter.

Table 2 lists the values of the parameters of these linear equations and the coefficients of determination. Replacing the equivalent equation for each fitting parameter in Eq. 1, the following expression is obtained.

$$h(t) = (a_0 + b_0 \cdot w_{PCM}) \cdot \left[1 - e^{-\frac{t-(a_1+b_1 \cdot w_{PCM})}{a_2+b_2 \cdot w_{PCM}}} \right] \quad (4)$$

Results shown in Fig. 4 illustrate the good agreement between experimental data and those predicted by Eq. 4 with an average error below 3.5%. Thus, Eq. 4 allows us to predict the growth of the foam as a function of time and microcapsules content.

Density

Densities of the foams depending on the foam zone and the microcapsules content are shown in Table 3. As can be seen, the foam exhibits a higher density at the bottom and it decreases as the foam grows up. As expected, the foam density increases with microcapsule content. It is important to point out that the Spanish regulations for the use of foams in building applications (UNE 92120) specify that the density of RPU foams should be higher than 30 kg/m^3. According to these results, all synthesized foams satisfied this restriction, being improved with the microcapsules addition. The theoretical density was calculated by considering the mass added and the final volume. The difference between the theoretical and the experimental foam density was negligible for the foam without microcapsules, whereas this difference increases with microcapsules content as expected because of certain CO_2 losses produced during the formation of the foam structure [2].

Table 3 Densities of the foams containing microencapsulated Rubitherm® RT27

Density (kg/m^3)				
Foam	0%	11%	18%	21%
Zone 1	34.30	37.70	43.48	63.50
Zone 2	34.02	36.80	41.13	49.22
Zone 3	33.41	33.82	40.1	47.29
Global	33.91	35.78	41.29	52.04
Theoretical	33.52	40.34	47.80	56.34
Exp. and theo. deviation (%)	1.14	12.74	15.77	8.26

Microcapsules distribution

Table 4 lists the latent heat values at different points of the foams obtained by DSC analysis. These results reveal the presence of microcapsules distributed by the whole foam because all the analyzed samples showed a TES capacity

Table 4 TES capacity of the foams with microencapsulated Rubitherm® RT27

Point of analysis	TES capacity (kJ/kg)		
	11%	18%	21%
Zone 1			
1	14.41	13.72	23.37
2	10.79	12.40	16.38
3	5.25	12.04	17.15
4	7.08	14.18	8.05
Global Zone 1	9.38	13.09	12.24
Zone 2			
5	11.15	12.16	10.28
6	8.50	20.72	19.48
7	8.27	11.99	25.05
8	4.28	20.15	20.39
Global Zone 2	8.05	16.26	18.80
Zone 3			
9	6.69	12.91	27.05
10	8.10	14.39	13.77
11	10.46	9.34	16.60
12	4.66	15.63	22.45
Global Zone 3	7.48	13.07	19.97
Average experimental TES (kJ/kg)	8.18	14.11	18.35
Average theoretical TES (kJ/kg)	8.28	14.00	17.55
Exp. and theo. deviation (%)	1.24	0.76	4.28

higher than that of the pure foam. This result takes place because the particle size of the incorporated microcapsules is below 2 μm (Fig. 5) which is really low compared with the size of the analyzed specimen (5.0 mm of side approximately). Nevertheless, a high variation can be found between the latent heat of the different analyzed samples in the defined zones; that can be attributed to the constraint in the sample size required by the DSC equipment. In order to avoid the effect of the sample size, an average latent heat was considered for the different foam zones. Contrary to the individual points, the study of the foam latent heat by zones indicates that the microcapsules distribution and the synthesized foam can be considered homogeneous.

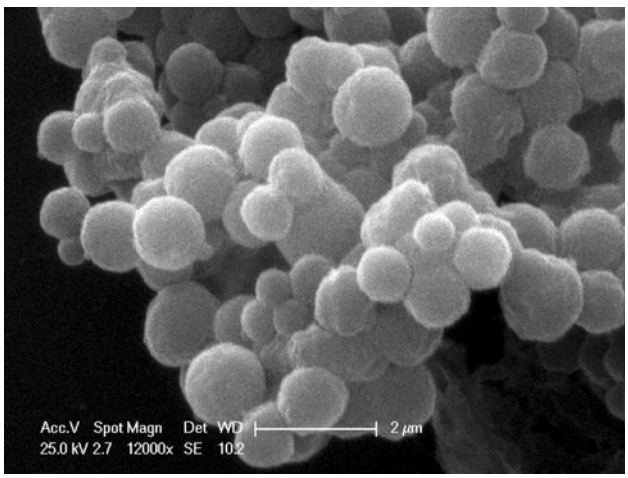

Fig. 5 SEM picture of the microcapsules containing PCMs incorporated in the PU foams (×12,000)

The theoretical and experimental average TES of the foams were calculated by means of Eqs. 5 and 6, respectively.

$$\Delta H_{FPCMs_{Teo}} = \frac{\Delta H_{mPCMs} \cdot W}{FW} \tag{5}$$

$$\Delta H_{FPCMs_{exp}} = \frac{\sum_{i=1}^{3} \overline{\Delta H_i} \cdot V_i \cdot \rho_i}{\sum_{i=1}^{3} V_i \cdot \rho_i} \tag{6}$$

where ΔH_{mPCMs} is the microcapsule latent heat, $\Delta H_{FPCMs_{Teo}}$ is the theoretical foam latent heat, W and FW are the microcapsules and foam weights, respectively, $\overline{\Delta H_i}$ is the average latent heat for each zone, $\Delta H_{FPCMs_{exp}}$ is the experimental latent heat, V_i is the volume and ρ_i is the density of each zone and i is a counter of the number of foam zones.

The good agreement between the theoretical and experimental latent heat values, with average deviations lower than 5%, indicated that DSC analysis is not necessary to obtain TES capacity, because the theoretical calculation is good enough. On the other hand, the average TES capacity obtained for the foam containing a 21 wt% of microcapsules is close to the maximum TES capacity of 18 J/g reported by You et al. [7] for foams with microencapsulated *n*-octadecane contents higher than 22 wt%.

SEM analysis

The structures of RPU foams obtained by SEM with magnification 50× are shown in Fig. 6. As can be seen, the foam cell sizes and its structure depend on the microcapsules content. Figure 6a obtained for the foam without microcapsules indicates that the RPU foams exhibit polyhedral closed-cell structures with pentagonal or hexagonal faces containing nodes formed by the junction of four struts, three in the micrograph plane and other out of the plane. Nevertheless, when 11 wt% of microcapsules was added (Fig. 6b), the closed cells tend to be spherical and of smaller size. On the other hand, Fig. 6c and d shows foams containing 18 and 21 wt% of microcapsules, respectively. Here, the foam cells had the shape of large polygons that seem to be formed by the rupture of struts especially for the highest microcapsule contents. These broken struts would

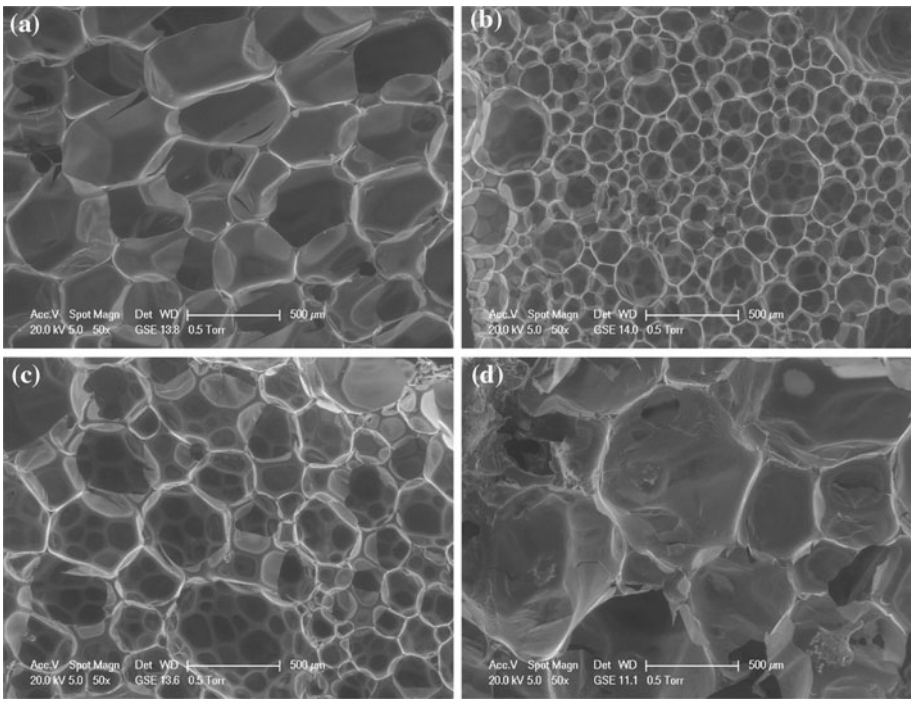

Fig. 6 SEM pictures with magnification ×50 of PU foams with different microcapsules loadings **a** 0 wt%, **b** 11 wt%, **c** 18 wt%, **d** 21 wt%

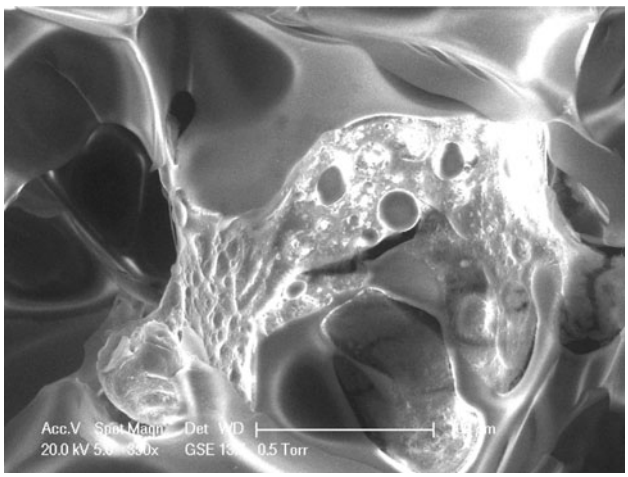

Fig. 7 SEM picture with magnification ×350 of a broken strut of the RPU foam with 11 wt% microcapsules containing PCMs

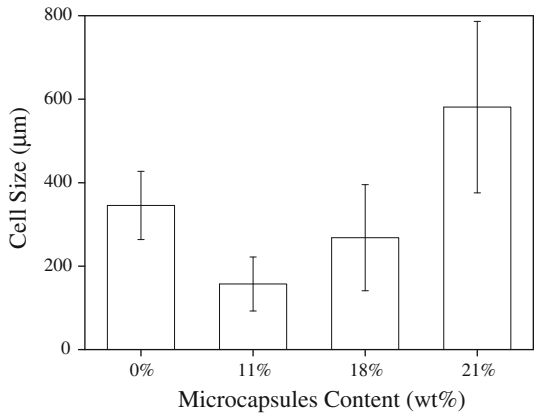

Fig. 8 Cell size of the PU foams as a function of microcapsules content

explain the large reduction in the final foam height as result of the carbon dioxide that escapes from these broken cells.

Figure 7 shows the SEM picture of a broken strut of the RPU foam with 11 wt% PCM at a SEM magnification 350×. This result confirms the presence of microcapsules inside the strut and also, that microcapsules do not change during the foaming process according to Fig. 5. The microcapsules location inside the strut indicates that a higher amount of microcapsules could cause the rupture of the strut.

The Image plus program was used to know the effect of the microcapsules content on the internal characteristics of the foam. The average cell sizes of the foams are shown in Fig. 8. As can be seen in this figure, the average cell size for a RPU foam without PCMs (345.3 μm) was larger than the obtained values for the foams containing 11 and 18 wt% PCM (157.2 and 266.1 μm, respectively) but lower than that for the foam containing 21 wt% PCM (590 μm). Foams with 11 and 18 wt% of microcapsules exhibits a lower cell size than those without fillers. It can be due to the increase in density and viscosity that controls the expanding structure [9, 14]. Similar results were reported by Cao et al. [15], Lee et al. [16] and Saint-Michel et al. [17]. They observed smaller cell sizes promoted by fillers, acting as a nucleation agent during cell formation. On the other hand, the largest cell-size obtained by the foam containing 21 wt% of microcapsules can be due to the

struts rupture during the foaming process, which gives place to the formation of struts of larger length.

Compression test

The best shape of the foam cells was obtained for the foam with 11 wt% of microcapsules, which has the lowest cell size. It could be expected that the lower foam cell sizes, the higher mechanical strength, as their struts and edges would be thicker. Therefore, an additional foam with a microcapsules content between 0 and 11 wt% was studied.

It is well known that the mechanical properties of a RPU foam is strongly dependent on its density [9, 18]. As aforementioned, foam densities were dependent on the foam filler content. Therefore, reduced compressive strength (RS) and modulus (RE) were calculated by dividing S and E by the sample density, excluding the density effects on these mechanical properties. Figure 9 shows the RS and RE of the synthesized foams as a function of the fillers content. RS results (Fig. 9a) indicated that there was no significant difference between the RS of foams containing 0 to 5 wt% of microcapsules (3.85 and 3.59 MPa/g/cm^3, respectively). However, this strength decreases sharply when the microcapsule content is increased up to 11 wt% (1.40 MPa/g/cm^3). Similar results were obtained by Mahfuz et al. [19] when a low density filler such as SiC was used, observing that a high percentage of this filler decreases the foam mechanical properties. This can be due to the high particle-to-particle interactions that appear at high filler contents promoting the particle agglomeration, increasing the number of collapsed cells and reducing the mechanical strength. In the same way, the RS for RPU foams can be modified by changing the polyol type and the foam recipe, finding reported values between 0.2 and 8 MPa/g/cm^3 [15, 16, 18]. Thus, all the synthesized foams exhibited a RS similar to those reported in literature, with foam densities in the range of the values required by the Spanish Regulation for building applications.

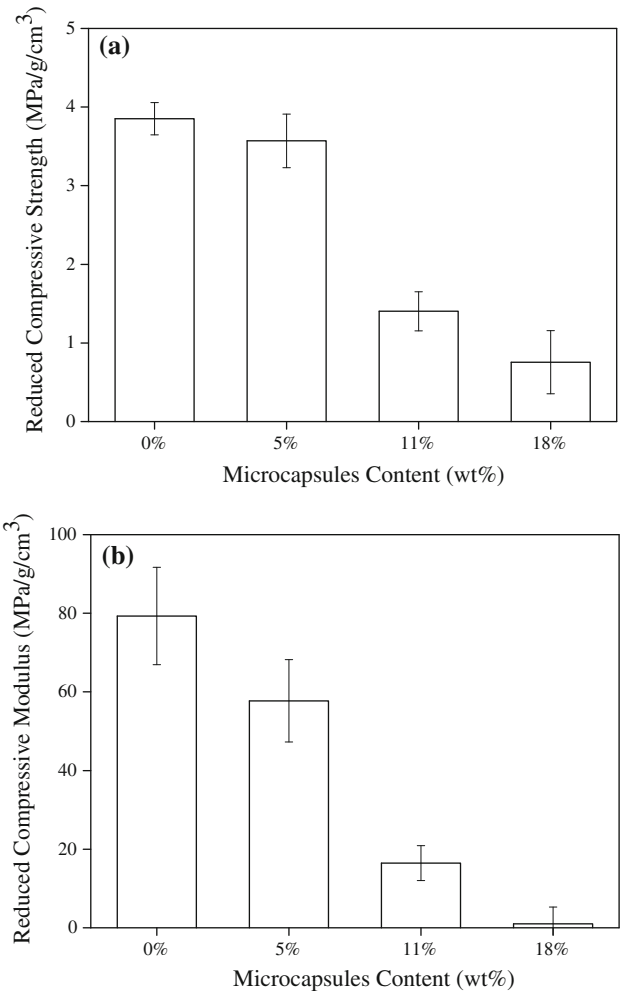

Fig. 9 Mechanical properties of PU foams incorporating different microcapsules contents: **a** RS, **b** RE

RE results shown in Fig. 9b indicated that the foam stiffness decreased with the microcapsule content. This behaviour can be explained taking into account that higher filler contents lead to more microcapsules being positioned into the struts, promoting the rupture of cells and decreasing its stiffness. This behaviour was more abrupt for the analyzed foam specimens having a filler content higher than 5 wt%. In the same way that for RS, RE results are in the range of those reported in literature (2–200 MPa/g/cm^3) [15, 16, 18]. Thus, the higher foam microcapsules content, the lower mechanical resistance and stiffness of the foam.

Conclusions

A 21 wt% content of microencapsulated Rubitherm® RT27 can be incorporated in RPU foams, improving the TES capacity of these materials but depressing their mechanical properties. Results indicated that the foaming process was affected by the microcapsules content decreasing the foam rising rate and its final size. The proposed model of first-order with dead time allowed to predict the foam height as a function of time and the microcapsule content. DSC analysis showed that the microcapsules were homogeneously distributed and SEM images illustrated that the microcapsules can be found either on the cells or forming part of the struts. In addition, these images indicated that the cells size and foam structure were dependent on microcapsules content, obtaining a minimum cell size for a content of 11 wt%.

Although the filler concentration decreased the mechanical properties, diminishing the reduced compressive

strength in a 7% and the modulus in a 25% for a microcapsules content of 5 wt%, values were in the range of those reported in literature for RPU foam containing other filler types. Besides, the foam densities satisfied the restriction established by the Spanish regulation for building applications.

Acknowledgements Financial support from Acciona Infraestructuras S.A., and the fellowship and grant from the Spanish Ministry of Science and Innovation are gratefully acknowledged. Ana M. Borreguero would like to acknowledge the help and support of Raquel Arévalo during her stay at Queen Mary University of London.

References

1. Sarier N, Onder E (2007) Termochim Acta 454:90
2. Wu J, Wang Y, Wan Y, Lei H, Yu F, Liu Y, Chen P, Yang L, Ruan R (2009) Int J Agric Biol Eng 2:40
3. You M, Zang XX, Wang JP, Wang XC (2009) J Mater Sci 44:3141. doi:10.1007/s10853-009-3418-7
4. Borreguero AM, Carmona M, Sánchez ML, Valverde JL, Rodríguez JF, (2010) Appl Therm Eng. doi:10.1026/applthermaleng.2010.01.032
5. You M, Zhang XX, Li W, Wang XC (2008) Thermochim Acta 472:20
6. Ye L, Meng XY, Ji X, Li ZM, Tang JH (2009) Polym Degrad Stabil 94:971
7. You M, Wang X, Zhang X, Li W (2008) Mod Appl Sci 2:44
8. Gravalos J, Calvo I, Mieres J, Cubillo J, Borreguero AM, Carmona M, Rodriguez JF, Valverde JL (2009) Patent EP2119498 (A1)
9. Verdejo R, Stämpfli R, Alvarez-Lianez M, Mourad S, Rodriguez-Perez MA, Brühwiler PA, Shaffer M (2009) Compos Sci Technol 69:1564
10. Marciano JH, Rojas AJ, Williams JJ (1982) Polymer 23:1489
11. Li S, Vatanparast R, Lemmetyinen H (2000) Polymer 41:5571
12. Seo D, Youn JR (2005) Polymer 46:6482
13. Marlin TE (2000) Process control designing processes and control systems for dynamic performance, 2nd edn. McGraw-Hill, Toronto
14. Dawson JR, Shortall JB (1982) J Mater Sci 17:220. doi:10.1007/BF00809056
15. Cao X, Lee LJ, Widya T, Macosko C (2005) Polymer 46:775
16. Lee LJ, Zeng C, Cao X, Han X, Shen J, Xu G (2005) Compos Sci Technol 65:2344
17. Saint-Michel F, Chazeau L, Cavaillé JY (2006) Compos Sci Technol 66:2709
18. Tanaka R, Hirose S, Hatakeyama H (2008) Bioresource Technol 99:3810
19. Mahfuz H, Rangari VK, Islam MS, Jeelani S (2004) Compos A Appl Sci Manuf 35:453